Supplementary Information has two parts:

1) Supplementary Videos S1-S2 show excerpts of C57BL/10, *mdx*, C57BL/6, and *Sgca*-null mice pre- and post-exercise in QuickTime movie (.mov) format. Each movie clip is approximately 7 MB.

Kobayashi-Nature movie S1a. Pre-exercise activity of a C57BL/10 wild-type mouse

Kobayashi-Nature movie S1b. Pre-exercise activity of an *mdx* mouse

Kobayashi-Nature movie S1c. Pre-exercise activity of a C57BL/6 wild-type mouse

Kobayashi-Nature movie S1d. Pre-exercise activity of an *Sgca*-null mouse

Kobayashi-Nature movie S2a. Post-exercise activity of a C57BL/10 wild-type mouse.

Kobayashi-Nature movie S2b. Post-exercise activity of an *mdx* mouse

Kobayashi-Nature movie S2c. Post-exercise activity of a C57BL/6 mouse wild-type mouse

Kobayashi-Nature movie S2d. Post-exercise activity of an *Sgca*-null mouse

2) Supplementary Figures S1-S7 – This file is a single PDF file that contains Full Methods, embedded Figures S1-S7 with Figure legends, and a Supplementary Table 1, along with additional Methods, References, Discussion and Acknowledgements for Supplementary Information. The Supplementary information presents additional material supporting conclusions and interpretations in the main text.

Kobayashi-Nature Figure S1. MCKeSG/*Sgca*-null mouse

Kobayashi-Nature Figure S2. Microdystrophin/*mdx* DGC

Kobayashi-Nature Figure S3. Vascular narrowings after exercise

Kobayashi-Nature Figure S4. *nNOS*-null mice after mild exercise

Kobayashi-Nature Figure S5. *mdx*;*nNOS*-null vertical activity

Kobayashi-Nature Figure S6. Percent vertical activity loss post-exercise

Kobayashi-Nature Figure S7. PDE5A inhibitor treatment

Kobayashi-Nature Figure S8. No edema in MRI views of hind-leg muscles

Kobayashiy-Nature Figure S9. nNOS is reduced in human muscle diseases

Supplementary Table 1. Summary of 425 human muscular biopsies stained for nNOS

Supplemental information - ADDITIONAL METHODS

Mouse models. Mouse strains obtained from Jackson Laboratories: C57BL/6, C57BL/10, *mdx*/C57BL/10ScSn, *nNOS*-null, and *eNOS*-null. Microdystrophin/*mdx* mice were described previously[1, 2]. Mice were maintained at the University of Iowa Animal Care Unit in accordance with the institute's animal usage guidelines. We found that sarcolemmal nNOS in female C57BL/6 mice was less than or equal to that in their male counterparts, depending on the stage of the estrous cycle; since even ovariectomized rats[3] and ovariectomized mice lose sarcolemmal nNOS, we only tested males. All mice were 10 wks of age, unless otherwise stated. Genetically defined mice were randomized between cages to avoid bias and tested blindly. *Sgca*-null mice[4] were backcrossed to a C57BL/6 background (BC5). MCKεSG/*Sgca*-null mice were bred with the *Sgca*-null (BC5) line for 8 generations. EC-SOD mice were from J.D. Crapo's laboratory and expression was driven by the β-actin promoter; these mice were mated with *mdx* mice for two generations and tested. *Dtna*-null mice[5] were on a pure C57BL/6 background and were from Drs. R. Mark Grady and J.R. Sanes.

Exercise-activity assay. Mouse housing and exercise-activity rooms were under specific pathogen-free conditions. Since anesthesia causes alterations in blood glucose[6] as well as in the blood flow[7] to skeletal muscle, we designed our exercise-activity assay without anesthesia. Also, to reduce anxiety, which could potentially lead to increases in blood glucose, and to keep behavioral variables at a minimum, we tested mice that were not individually housed[8]. The same handler performed each assay. Mice were activity-monitored using the VersaMax Animal Activity Monitoring System from AccuScan Instruments, Inc. This system uses a grid of invisible infrared light beams that traverse the animal chamber front to back and left to right to monitor the position and movement of the mouse within an X-Y-Z plane. Activity was monitored over a 24 hour cycle to determine their most active time. All mice tested were synchronized to a shifted 12:12-hour light:dark cycle so that at the time of testing, the mice were behaviorally most active. Mice were acclimatized to the activity test room, which was on the same light:dark cycle, for at least an hour. Mice were tested in individual chambers in sets of 4, for 30 x 1 minute intervals pre- and immediately post-exercise, at the same time every day in the dark, in an isolated room, and with the same handler. Testing equipment was cleaned between each use to reduce mouse reactionary behavioral variables that could alter our results. Data collected was converted to a Microsoft Excel worksheet and all calculations were done within the Excel program. Zone map tracings were created by the AccuScan VersaMap-Zone mapping software where the X and Y plane represent the 2 dimensions of the activity chamber and the dots represent every time the mouse breaks the Z plane, registering vertical activity within the 30 minute time interval.

Animals were mildly exercised using an adjustable variable speed belt treadmill from AccuPacer (AP4M-MGAG, AccuScan Instruments, Inc.), down a 15° grade at 15 mpm for 10 minutes with acclimatization at 3 mpm for 5 minutes.

Antibodies. The nNOS antibody used for immunoblots and immunofluorescence was an affinity purified polyclonal antibody[9]. Antibodies for inflammation included: I-A^b MHC class II-conjugated to FITC and F4/80 conjugated to Alex Fluor® 647, both from

Invitrogen. For an atrophy marker, SC-71 antibody (ATCC) against myosin heavy chain 2A was used. For hypoxia and oxidative stress, polyclonal antibodies against HIF-1α (R&D Systems) and nitrotyrosine (Upstate), and Hypoxyprobe-1™ Mab1 conjugated to FITC (Chemicon® International) were used.

Immunoblotting analysis. Tissue for immunoblotting came from whole muscle and crude skeletal muscle membranes were prepared as follows: 1-3 g fresh hind leg skeletal muscle was homogenized in 7.5x volumes homogenization buffer (20 mM $Na_4P_2O_7$, 20 mM NaH_2PO_4, 1 mM $MgCl_2$, 0.303 M sucrose, 0.5 mM EDTA, pH 7.1 with 5 ug/ml Aprotinin and Leupeptin, 0.5 ug/ml Pepstatin A, 0.23 mM PMSF, 0.64 mM Benzamidine, and 2 uM Calpain inhibitor I and Calpeptin), then centrifuged 14k x g_{max}; supernatants were centrifuged 30k x g_{max}, after which pellets were resuspended in homogenization buffer. Homogenates and crude skeletal muscle membranes were prepared from different mouse models, run on SDS-PAGE and transferred to PVDF (Immobilon-P) transfer membranes for immunoblotting[10]. All immunoblotting was done by chemiluminescent detection using the Alpha Innotech imaging system.

Immunofluorescence analysis. Immunofluorescence staining for nNOS was performed on 7 μm transverse cryo muscle sections as described previously[9]. For patient biopsies, immunofluorescence staining was performed on serial cryosections; both anti-spectrin and anti-nNOS antibodies were purchased from Novocastra. For hypoxia analysis +/- exercise, Hypoxyprobe™ was injected 45 min before exercise.

Microfil® analysis of skeletal muscle vessels. Microfil® MV-130 Red (Flow Tech, Inc) was mixed according to manufacturer's instructions and perfused into the mouse aorta pre- or post-exercise at 100 mm Hg. After polymerization and clearing of skeletal muscles, vessels were imaged.

Tissue blood-flow mapping. The MoorLDI™ system using near infra-red wavelength laser (1.0 mm beam, 2.5 mW) doppler imaging without contrast was used to generate a color coded map of blood flow on a CCD camera at 72 x 582 pixel resolution. Range was at 20 cm distance in an area 5.1 cm x 4.2 cm at 182 x 152 resolution and scan speed of 4 ms/pixel.

Serum Creatine Kinase Assays. Blood for quantitative, kinetic determination of serum creatine kinase activity was collected either after the pre-exercise activity analysis or 2 hours post-exercise by mouse tail vein bleeds, using a Sarstedt microvette CB 300, from non-anesthetized restrained mice. Red cells were pelleted by centrifugation at 10,000 rpm for 4 minutes and serum was separated, collected and analyzed immediately without freezing. Serum creatine kinase assays were done with an enzyme-coupled assay reagent kit (Stanbio Laboratory) according to manufacturer's instructions. Absorbance at 340 nm was measure every 30 sec for 2 min at 37°C so that changes in enzyme activity could be calculated. Data were transferred to and calculated in a Microsoft Excel spreadsheet.

Contractile properties. Contractile properties were measured *in vitro* on extensor digitorum longus (EDL), soleus, or diaphragm muscles strips from C57BL/6, *mdx*,

MCKεSG/*Sgca*-null, MCKεSG, *Sgca*-null, or *nNOS*-null mice. Mice were anesthetized by an intraperitoneal injection (I.P.) of 2% avertin (0.0015 ml/g body weight). Supplemental injections were administered to maintain an anesthesia level that prevented responses to tactile stimuli. Intact muscles or DPM strips were removed from each mouse after the mice were euthanized by an overdose of avertin, and the thoracic cavity was opened. Muscles were immersed in an oxygenated bath (95% O_2, 5% CO_2) that contained Ringer's solution (pH 7.4) at 25°C. For each muscle, one tendon was tied securely with a 4-0 or 6-0 suture to a force transducer (one end), and a servo motor (other end). Using twitches with pulse duration of 0.2 ms, the voltage or current of stimulation was increased to achieve a maximum twitch and then increased slightly. Twitches were then used to adjust the muscle length to the optimum length for force development (L_o). The muscle length was set at L_o , and EDL muscles were stimulated for 300 ms, and soleus and DPM muscles for 900 ms. Stimulation frequency was increased until the force reached a plateau at maximum isometric tetanic force (P_o).

For C57BL/6, *mdx*, MCKεSG/*Sgca*-null, MCKεSG, *Sgca*-null mice, the susceptibility to contraction-induced injury was measured during two lengthening contractions, with the contractions separated by a rest interval of 10 s. Each contraction was initiated with the quiescent muscle set at L_o, and then a plateau at maximum force was produced by stimulating EDL muscles at a frequency of ~150 Hz for 150 ms and soleus and DPM muscles at ~120 Hz for 200 ms. While generating maximum force, the muscles were stretched through a 30% strain at a velocity of 1 Lf/s, and then returned to L_o. A measurement of P_o was made one minute later. Based on measurements of muscle mass, muscle length, fiber length, and P_o, the total fiber cross-sectional area and specific P_o (kN/m2) were calculated[1, 11]. The data were analyzed by an analysis of variance (ANOVA). When the overall F-ratio for the ANOVA was significant, the differences between individual group means were determined by a single t-test. Significance was set *a priori* at $P < 0.05$. Data are expressed as mean ± SEM.

Drug treatments. Timing and dosing of deflazacort was based on previous literature on *mdx* mice treated with deflazacort showing beneficial effects on *mdx* muscle pathology[12-15]. The steroidal anti-inflammatory Deflazacort (Axxora® Platform) was resuspended in DMSO at 36 mg/ml and then diluted 1:100 in 0.9% saline immediately prior to I.P. injection at 1.5 mg/kg/day for acute and 1.2 mg/kg/day for the 3-week chronic treatment. Timing and dosing of ibuprofen (Alpharma, Inc) was based on veterinary formularies for anti-inflammatory and analgesic doses and previous literature[16, 17]. Ibuprofen was in suspension and delivered orally at 50 mg/kg/day.

The nNOS inhibitor 3-bromo-7-nitroindazole (3-B-7-Ni) (Cayman Chemical) or the endothelin receptor type 1b agonist, sarafotoxin 6c (a vasoconstrictor peptide, Alexis Biochemicals), was resuspended in DMSO at 100 mg/ml and 1 mg/ml, respectively. 3-B-7-Ni was diluted 1:10 in sunflower oil and immediately injected at 20 mg/kg I.P. Sarafotoxin 6c was diluted 1:1000 in 0.9% saline and immediately injected at 5 ug/kg I.P.

In determining the dosage of PDE5A inhibitor, we wanted our dose of PDE5A inhibitor to give a good exposure to PDE5A, so we took into account the following points: a dose of 100 mg/kg/day will give a mean free plasma concentration of 10.4 nM[18-20] (the IC_{50} of sildenafil at PDE5A is 5-10 nM[19] thus 100 mg/kg/day is at the IC_{50} for sildenafil at PDE5A), PDE5 activity is elevated 2-6x in mouse leg muscle extracts from *mdx* mice[21],

and food-drug interactions reducing the rate of absorption and extent of systemic exposure for PDE5A inhibitors[18]. Doses of 100, 300, and 500 mg/kg/day were tested on *mdx* mice and 300 mg/kg/day gave the best response (see Figure S7d). Assuming linear pharmacokinetics from 100-300 mg/kg/day, 300 mg/kg/day will produce approximately a plasma concentration of 30 nM, exceeding the IC_{50} by 3-6 fold, inhibiting more than 50% of the enzyme activity. Therefore, for acute tadalafil (Kemprotec) treatment, tadalafil was given orally by gavage at 300 mg/kg the day before and the day of the exercise-activity protocol to ensure that the mice received one full day of inhibitor dosage before the exercise-activity protocol. For acute sildenafil citrate (Pfizer) treatment, sildenafil was given orally by mixing the drug into water softened rodent gruel (2019 Teklad global 19% protein rodent chow; 4-6 g/day). Mice were supplemented with normal chow (7013 NIH-31 modified diet) to ensure *ad libitum* feeding. For K_{ATP} channel agonists, stocks at 100 mg/ml of Minoxidil (Sigma) and pinacidil (Alexis Biochemicals) were resuspended in DMSO, and nicorandil (SynFine Research) was resuspended in water. Each drug was diluted in 0.9% saline immediately before i.p. injection, at 0.8 mg/kg in the case of minoxidil and pinacidil or 0.1 mg/kg in the case of nicorandil. L-NAME was given orally by gavage at 100 mg/kg in 0.9% saline the day before and the day of the exercise-activity protocol. Superoxide dismutase (Sigma) was given by i.v. at 1000 U/mouse. Tempol (Alexis Biochemicals) was delivered by i.p. at 260 mg/kg.

All agents were administered 30 minutes prior to exercise-activity analysis unless otherwise stated.

Magnetic resonance imaging (MRI). MRI was performed using a Varian Unity/Inova 4.7 T small-bore MRI system (Varian Inc., Palo Alto, CA). The acquisition consisted of a T2-weighted fast spin-echo sequence (TR/TE = 5000/48 ms) with in-plane resolution of 0.11 mm x 0.22 mm and slice thickness of 0.6 mm acquired in the axial plane. Imaging of mice was +/- exercise. For imaging, mice were anesthetized with an i.p. injection of ketamine/xylazine (87.5 mg/kg and 12.5 mg/kg, respectively). If with exercise, imaging started 30 minutes post-exercise. 4 *mdx* mice were imaged for pre-exercise and 7 *mdx* mice were imaged for post-exercise and 5 *mdx* were treated with PDE5A inhibitor. Three mice were examined for other sets. Measurements to determine percent muscle edema were done with Image-ProPlus6.0 Software. Axial or coronal muscle areas were measured and fat and cartilage were subtracted. Total areas of edema were measured within the same slice and divided by the resultant axial muscle area and multiplied by 100 to get percent muscle edema area for each mouse tested (Fig. 3g). The middle axial and coronal slices were used for this quantitation as these slices gave the greatest viewable muscle area per scan. Axial and coronal calculations gave similar and consistent percent muscle edema areas.

Statistical analysis. Unless otherwise stated, the data were calculated according to an analysis of variance. *P*-value calculations were made between genetically defined mouse models and their wild-type counterparts or between treated and untreated mice using the Kruskal-Wallis One Way Analysis on Ranks. Data are expressed as mean ± SEM.

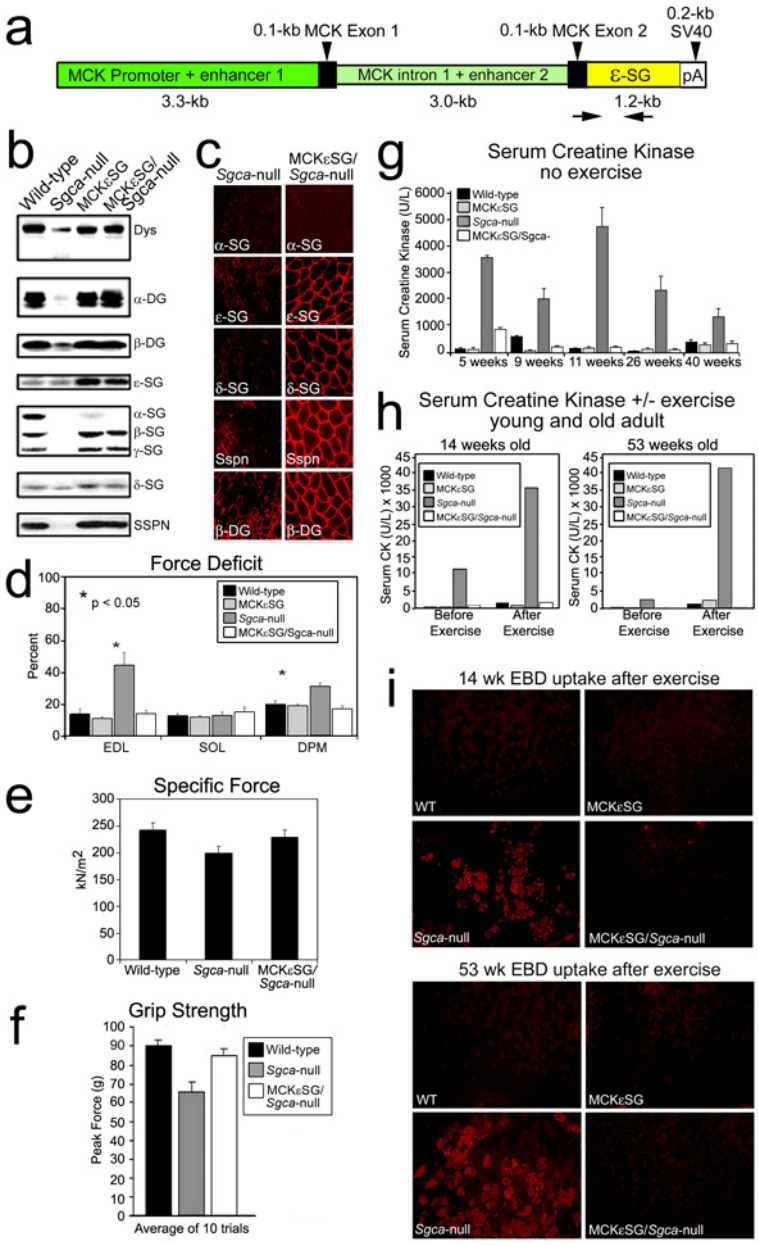

Figure S1 | Overexpression of ε-sarcoglycan in striated muscle of *Sgca*-null mice restores the DGC and normal muscle function. **a**, The mouse muscle creatine kinase promoter was used to drive transgenic expression of a human ε-sarcoglycan transgene in mice. Arrows indicate positions of primers used for genotyping. **b**, Immunoblotting for structural DGC components showed a complete recovery of the DGC in crude muscle membrane preparations from *Sgca*-null mice in which the ε-sarcoglycan transgene was expressed. Littermate wild-type, *Sgca*-null, and MCKεSG mice were used for a comparison of expression levels. **c**, Immunofluorescence detection of α-, ε-, δ-sarcoglycan, sarcospan, and β-dystroglycan in littermate 5-week old *Sgca*-null and MCKεSG/*Sgca*-null mouse quadriceps showing restoration of the sarcoglycans and sarcospan to the

sarcolemma, due to the expression of the ε-sarcoglycan transgene. Detection of β-dystroglycan was used as a control for membrane staining. **d**, Force deficit measurements of extensor digitorum longus (EDL), soleus, and diaphragm (DPM) muscles. All tests were performed on each of the 4 mouse strains with n=4 for each muscle of each strain. **e**, *In vitro* specific force measurements comparing wild-type, *Sgca*-null and MCKεSG/*Sgca*-null EDL muscles. **f**, Whole-mouse-grip strength force measurement comparing wild-type, *Sgca*-null and MCKεSG/*Sgca*-null forearm strength. **g**, Serum CK levels in unexercised mice, measured at different time points up to 40 weeks of age, showed MCKεSG/*Sgca*-null mice to have low CK levels that were similar to those of their littermate wild-type and MCKεSG controls, and much lower than those of *Sgca*-null littermate controls. **h**, Comparison of serum CK levels in 14- and 53-week old littermate wild-type, MCKεSG, *Sgca*-null, and MCKεSG/*Sgca*-null mice before and after exercise. **i**, Images of quadriceps muscle from each genotype, examined for Evans blue dye uptake, which indicates muscle fiber damage. (Error bars are S.E.M.)

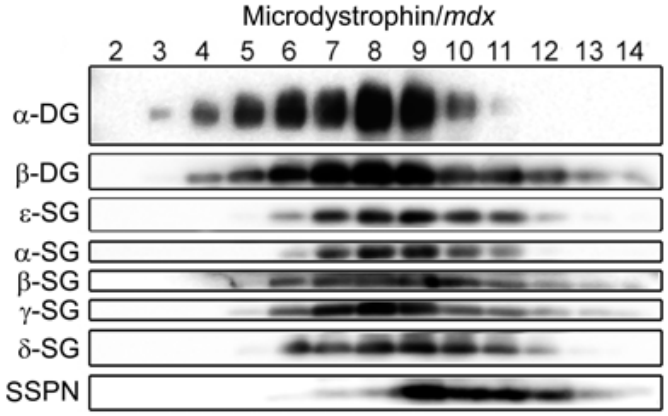

Figure S2 | Microdystrophin(udys)/*mdx* skeletal muscle DGC is intact. A sucrose density gradient of skeletal muscle DGC from microdystrophin/*mdx* mice, showing a structurally intact DGC – α- and β-dystroglycan (α-DG and β-DG), α/ε-sarcoglycan (α/ε-, β-, γ-, and δ-SG), and sarcospan (SSPN). In *mdx* mice, the DGC structural components are dispersed through the sucrose gradient[22].

Microdystrophin/*mdx* mice show restoration of the structural DGC proteins to the sarcolemma, with contractility returning to the levels seen in wild-type mice[1] but, as we show in Figure 1e, without restoration of nNOS to the sarcolemma. We also show in Figure 1e that microdystrophin/*mdx* mice have excessive inactivity after mild exercise, despite contractility being normal.

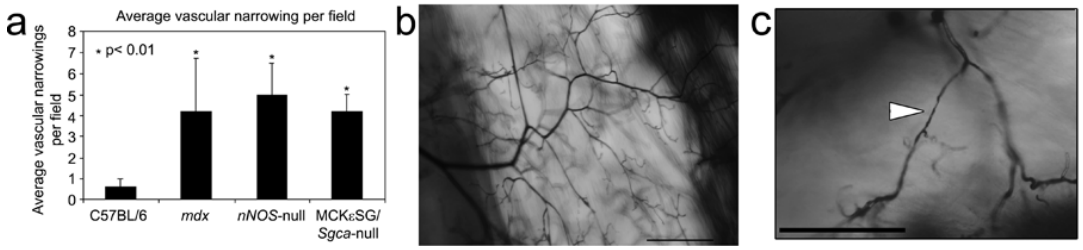

Figure S3 | Vascular narrowings after exercise. **a**, Skeletal muscle vascular narrowings were averaged per field after exercise and compared to wild-type mice. After exercise, C57BL/6 mice have increased capillary perfusion and little to no vascular narrowings (**b**) whereas *mdx* (**c**), MCKεSG/*Sgca*-null, and *nNOS*-null mice do not (see Figure 1g and 2c). Each Microfil® image is a representative view of skeletal muscle vessels post-exercise. Arrowhead indicates narrowing. (Error bars = SEM, scale bar = 100 μm)

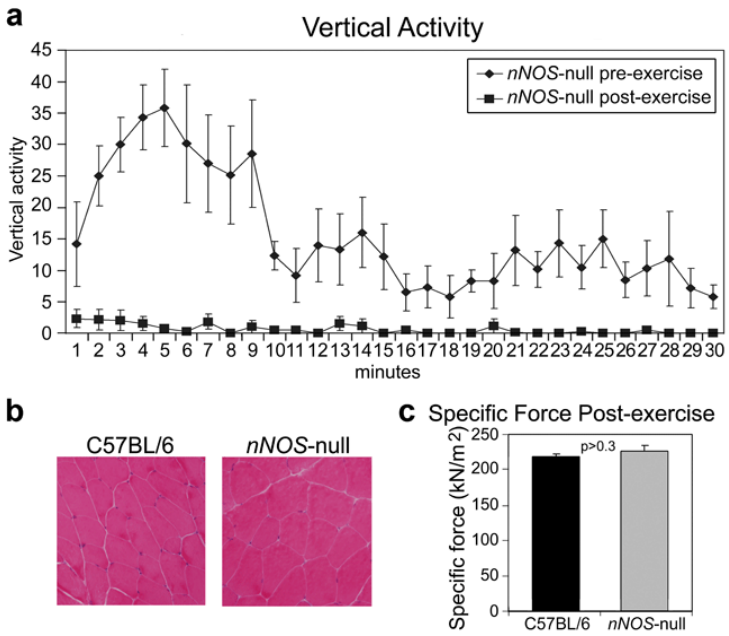

Figure S4 | *nNOS*-null mice after mild exercise. a, Charting of vertical activity for 30 minutes pre- and post-exercise showing that following a light bout of activity, the vertical activity in *nNOS*-null mice is extremely low throughout the entire 30 minute analysis. (n=4 for each). (Error bars are S.E.M.). **b**, Comparison of hematoxylin and eosin staining of quadriceps muscle sections from C57BL/6 and *nNOS*-null mice (n=6 for each) showing no signs of muscle pathology. **c**, Contractility comparison measuring specific force after mild exercise in C57BL/6 and *nNOS*-null EDL muscles (n=5 for each).

The exaggerated fatigue response to mild exercise is not muscle weakness. Evidence from mouse models demonstrates that reduced sarcolemmal nNOS does not affect muscle contractility: microdystrophin/*mdx*[1], MCKεSG/*Sgca*-null, and α1-*syntrophin*-null[23] mice have mislocalized nNOS but this does not influence contractile properties. In addition, *nNOS*-null muscles produce force comparable to, or even greater than, the force generated by wild-type muscle at different oxygen tensions[24]. To further test if loss of nNOS affects contractility, we exercised a set of *nNOS*-null mice, waited 10 minutes, which was within

the 30 minute time interval we used to assess the fatigue response after mild exercise (Supplemental Fig. S3), and put them on the treadmill again. The mice were able to run the full running protocol again indicating that they were still capable of performing physical activity and that the activity was not exhaustive. Our *nNOS*-null mouse data show that loss of nNOS-derived NO signaling leads to prolonged exercise-induced inactivity similar to that identified in our dystrophic and rescue mouse models.

In the mouse models with the fatigue response to mild exercise, full activity returned, and vascular narrowing were not present 4 hours after exercise indicating that the vascular narrowing as well as loss of activity post-exercise is not sustained. Vascular narrowings and the fatigue response occur again upon re-exercising of mice.

Non-selective NOS inhibitor data are consistent with our results from the treatment of wild-type mice with the relatively specific nNOS inhibitor 3-bromo-7-nitroindazole: treatment of wild-type mice with L-NNA prevents adequate exercise-induced hyperemia and limits exercise capacity during exhaustive treadmill running[25]; treatment of wild-type and *mdx* mice with L-NAME increases mean arterial pressure and decreases femoral blood flow velocity and vascular conductance[26]; L-NAME treatment severely reduces walking speed in rats[27], and local intra-arterial infusion of L-NMMA into human forearm reduces resting blood flow and a transient systemic increase in blood pressure[28]. We found that treatment of wild-type mice with L-NAME reduced post-exercise activity to levels similar to those in *nNOS*-null mice post-exercise, and that treatment of dystrophic or *nNOS*-null mice with L-NAME reduced the activity post-exercise even more, in fact preventing Microfil® from circulating sufficiently for images to be taken (data not shown). The L-NAME results are also consistent with our sarafotoxin 6c treatment of wild-type mouse data. In addition, the NOS inhibitor and sarafotoxin data are consistent with the fact that deflazacort treatment of *mdx* mice did not ameliorate inactivity post-exercise as glucocorticoids reduce inflammation by causing vasoconstriction to reduce blood flow and thus reducing permeability between the endothelial cells[29].

The exaggerated fatigue response to mild exercise is not due to oxidative stress, inflammation, or atrophy. To test the possibility that an inhibition of mitochondrial respiration inhibition causes the observed post-exercise inactivity, we tested *mdx* mice treated with superoxide dismutase (SOD) or *mdx* mice overexpressing the extracellular superoxide dismutase (under the β-actin promoter) in our exercise activity assay. We found that neither method of SOD exposure had an effect on the exaggerated fatigue response to mild exercise. In addition, since reactive oxygen species (ROS) increases the protein nitrosylation, we treated *mdx* mice with Tempol, a water-soluble, membrane permeable scavenger of superoxide anions that also reduces hydroxyl radical formation, and found that the drug had no effect on the exaggerated fatigue response in *mdx* mice. Furthermore, immunohistochemistry for nitrotyrosine in muscle sections of wild-type, rescue, or *nNOS*-null mice showed no changes +/- exercise.

We next probed for the expression of HIF-1α, an oxygen-dependent transcription activator that accumulates during oxidative stress, on skeletal muscle sections and on immunoblots of skeletal muscle homogenates, in wild-type, *mdx*, rescue, and *nNOS*-null mice before and after mild exercise, and did not detect any changes compared to levels in wild-type muscle. We also examined tissue hypoxia +/- exercise in wild-type, rescue, and

nNOS-null mouse models by injecting Hypoxyprobe™-1 and probed for hypoxyprobe adducts. We did not find signs of skeletal muscle hypoxia after the mild exercise.

On muscle sections of the non-dystrophic mouse models that displayed the exaggerated fatigue response, we probed for inflammation using I-A^b MHC class II and F4/80, and did not detect inflammation. To test for atrophy, we probed for myosin heavy chain 2A, and did not detect any signs of atrophy.

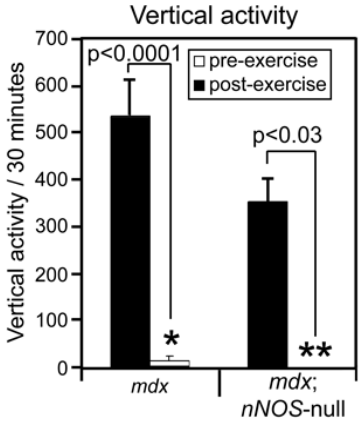

Figure S5 | *mdx*;*nNOS*-null mice and vertical activity. The exercise-induced vascular effect suggests that if nNOS were genetically deleted in a muscular dystrophy mouse model, the exercise-induced fatigue would be more significant. We tested this hypothesis by breeding the *mdx* and *nNOS*-null mice and analyzing the resulting *mdx*;*nNOS*-null mice in our exercise-activity assay. We found that the *mdx*;*nNOS*-null mice (n=4) had even less vertical activity pre- and post-exercise than their *mdx* littermates (*mdx*;$nNOS^{+/-}$ or *mdx*;$nNOS^{+/+}$)(n=7).

Loss of nNOS in *mdx* mice does not exacerbate muscle damage but will increase the exaggerated fatigue response to mild exercise. Comparative analyses of muscle pathology in *mdx*/*nNOS*-null mice versus *mdx* mice have led to the conclusion that *mdx* dystrophic pathology is independent of nNOS perturbation[9, 30]. However, fatigue was not analyzed in the *mdx*/*nNOS*-null mouse studies, and these mice were not challenged with exercise to test the repercussions of complete loss of nNOS in *mdx* muscle. On the other hand, NOS-Tg/*mdx* mice, which overexpress nNOS in *mdx* muscle, showed an amelioration of common indices of muscle pathology, due to reduced inflammation and membrane injury[31]. These mice, however, in spite of a 50-fold increase in nNOS protein in transgenic muscle, have only ~0.2 fold increase in NO production. This finding is reminiscent of the up-regulation of nNOS in DMD myofibers, which is accompanied by low NO levels[32]. The low NO production in NOS-Tg/*mdx* mice was attributed to possible increased expression of NOS inhibitors. However, this study did not confirm the localization of the overproduced nNOS protein, analyze fatigue, or challenge the NOS-Tg/*mdx* mice to analyze the effects of the 50-fold increase in nNOS expression in *mdx* mice.

Our muscle nNOS data are consistent with recent evidence showing that a structurally intact DGC in smooth muscle only partially restores α-adrenergic vasoregulation in *mdx* hindimbs[21], suggesting an extrinsic vascular contribution to vasomodulation. Importantly, we only see the vascular constrictions in the skeletal muscle

vasculature post-exercise in the *mdx*, *Sgca*-null, *nNOS*-null, and rescue mice. We did not detect vascular narrowing in other organs.

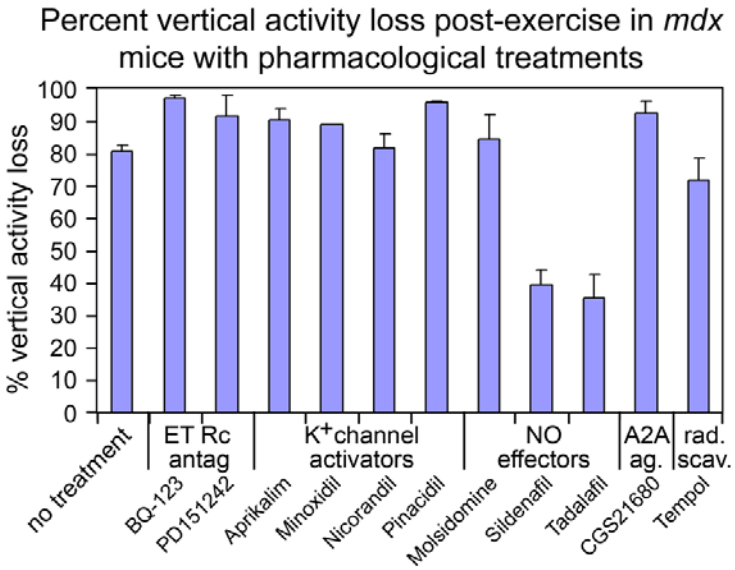

Figure S6 | Percent vertical activity loss post-exercise in *mdx* mice treated with different classes of pharmacological vasodilators. The loss of post-exercise vertical activity in *mdx* mice was quantified with and without treatment with various classes of vasodilators. The drugs tested were: ET_a receptor antagonists BQ-123 (0.1 mg/kg, n=3), and PD151242 (25 ug/mouse, n=4); the potassium channel activators Aprikalim (400 uM/mouse, n=4), Minoxidil (0.8 mg/kg, n=2), Nicorandil (0.1 mg/kg, n=2), and Pinacidil (0.8 mg/kg, n=2); the NO level activators Molsidomine (125 ug/mouse, n=4), Sildenafil (300 mg/kg, n=4), and Tadalafil (300 mg/kg, n=6) (note sildenafil and tadalafil affect cGMP levels, downstream of NO); the adenosine 2A receptor antagonist CGS21680 (1 ug/kg, n=2); and the superoxide scavenger Tempol (260 mg/kg, n=4). Untreated control mice for each drug class were pooled, resulting in n=34. Error bars are S.E.M.

The vasodilators bypass the nNOS-NO-cGMP mechanism and stimulate general vasodilation. While this would prevent vasoconstrictions like those seen with verapamil in sarcoglycanopathy mouse models[33], the bypass also eliminates the mechanism of nNOS stimulation by muscle contraction. Thus, the animals become hypotensive upon exercise and more inactive. For example: mice treated with minoxidil have catecholamines released into their bloodstream – a baroreflex-mediated response to low blood pressure[34]; nicorandil dilates peripheral and coronary resistance arterioles, systemic veins, and epicardial coronary arteries, thus significantly reducing blood pressure in mammals[35], and pinacidil decreases mean arterial pressure in wild-type mice[36].

Our data show that the exercise-induced prolonged fatigue response is alleviated by PDE5A inhibitor treatment, indicating that the effect we see is due to cGMP, which acts downstream of NO production. Downstream effects of low, physiological levels of NO (e.g. mitochondrial biogenesis and vasodilation) are cGMP-dependent, whereas downstream effects of high (pathological) NO levels (e.g. generation of reactive oxygen species and nitrosylation of proteins, lipids, and DNA) are cGMP-independent.[37]

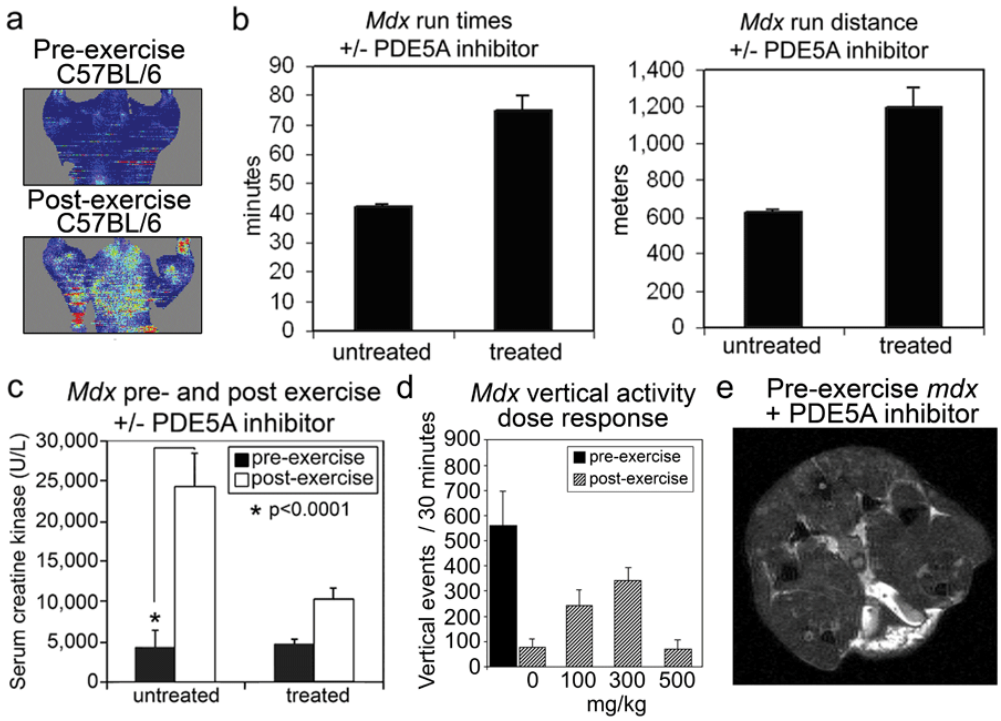

Figure S7 | PDE5A inhibitor treatment. a, Representative images of coronal Laser Doppler analysis of blood flow from C57BL/6 mice pre- and post-exercise (compare with Fig. 3a-b), b, *Mdx* mouse run times and run distances +/- PDE5A inhibitor treatment. **c**, *Mdx* pre- and post-exercise serum creatine kinase levels +/- PDE5A inhibitor treatment. (n=6 and error bars are S.E.M.) **d**, *Mdx* dose-vertical activity response curve to PDE5A inhibitor. (untreated n=6, 100 mg/kg n=3, 300 mg/kg n=6, 500 mg/kg n=3, error bars are S.E.M.), **e**, representative axial MRI view of pre-exercised *mdx* + PDE5A inhibitor.

Consistent with PDE5A inhibitor treatment attenuating muscle damage in *mdx* mice[21], we found that this treatment also reduced the rise in post-exercise serum creatine kinase and increased the time and distance of running of the *mdx* mice tested.

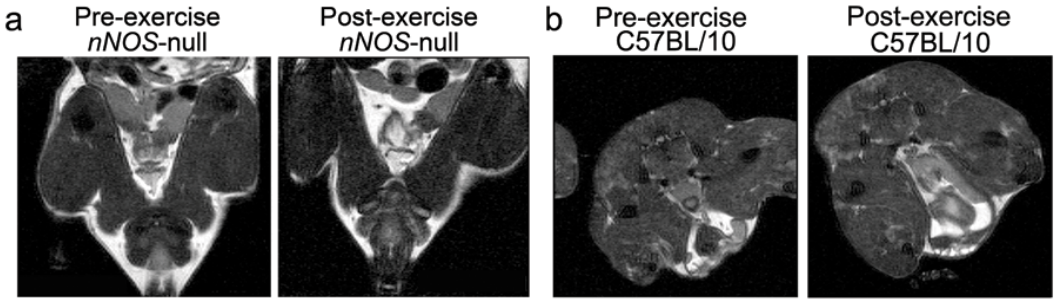

Figure S8 | No edema pre- and post-exercise in representative MRI views. **a**, Coronal views of *nNOS*-null hind-legs pre- and post-exercise (n=3), **b**, Axial views of C57BL/10 hind-legs (n=3) (0.70% +/- 0.50) (Compare to Fig. 3d-f),

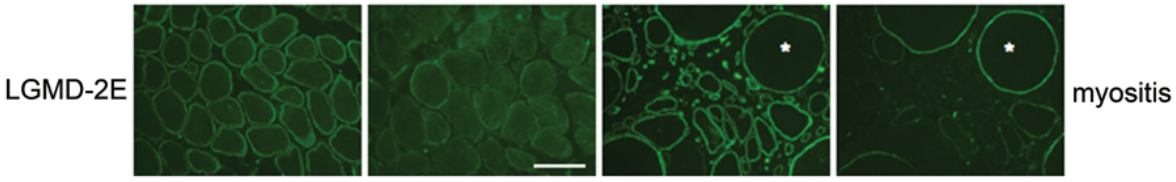

Figure S9 | nNOS is reduced in human muscle diseases. Additional example of a limb-girdle muscular dystrophy (LGMD-2E) and a non-dystrophic myopathy like polymyositis (myositis). Asterisks mark the same muscle fiber in some of the adjacent panels. (Compare to Fig. 4) (Scale bar = 100 um)

Table 1. Summary of the 425 human muscular biopsies stained for nNOS.

Disease	nNOS-negative	nNOS-reduced	nNOS-normal	Total cases stained
DMD	27	0	0	27
BMD	20	10	0	30
DMD carriers	Mosaic of negative and positive fibers			4
CMD/LGMD (POMT1, POMT2, POMGnT1, FKTN)	2	8	0	10
Other dystroglycanopathies not genetically defined	7	76	8	91
LGMD-2A	0	0	1	1
LGMD-2B	0	10	2	12
LGMD-2D	0	3	0	3
LGMD-2E	0	2	0	2
LGMD-2I	0	9	1	10
Other SG (includes three 2C cases)	0	6	0	6
UCMD	3	21	1	25
MDC1A	1	3	1	5
Myositis	2	6	0	8
Autophagic vacuolar myopathy	0	5	0	5
Myopathies w/o specific protein deficiencies	0	100	86	186

METHODS FOR SUPPLEMENTARY INFORMATION

Construction of transgene, transgenic mice, and MCKεSG/*Sgca*-null rescue mice. To direct skeletal and cardiac muscle-specific expression of ε-sarcoglycan in mice, an MCKεSGpA transgene was constructed: a 5' blunt-ended *Cla*I–3' *Xho*I fragment of the murine muscle-specific creatine kinase (MCK) 6.5-kb promoter/enhancer[38], was ligated into pGem7Zf(+) (Promega) 5' blunt-ended *Aat*II–*Xho*I sites. The full-length human ε-sarcoglycan cDNA (human and mouse ε-sarcoglycan are 96% identical) was PCR synthesized from a human skeletal muscle cDNA library (Clontech) and engineered with 5' *Xho*I–3' *Kpn*I sites then ligated downstream of the MCK promoter. An SV40 polyadenylation signal was PCR engineered with 5' *Kpn*I–3' HindIII/NruI/SacI linker and the *Kpn*I-*Sac*I fragment was ligated downstream of the ε-sarcoglycan coding region. All constructs were confirmed by DNA sequencing by the University of Iowa DNA Facility. The MCKεSGpA *EcoR*V–*Nru*I 7,986-bp transgene was microinjected by the University of Iowa Transgenic Animal Facility. Founder mice were identified, genotyped, and confirmed by PCR reactions of mouse genomic DNA isolated from tail or ear-snips[39]. Injection of the transgene yielded 3 independent germ line-transmitting founders, which were backcrossed to the C57BL/6 background to generate stable MCKεSG transgenic lines, and offspring were subsequently genotyped by PCR. Skeletal muscles from subsequent generations of transgenic mice were analyzed by SDS-PAGE to check for consistent expression of the transgene. MCKεSG/*Sgca*-null mice were generated by two rounds of breeding with *Sgca*-null mice[40] on a congenic C57BL/6 background. Offspring were PCR-genotyped for transmission of the transgene and loss of the corresponding allele.

Immunoblotting, immunofluorescence and histological analysis. Antibodies for immunoblots were MANDRA1 (dystrophin, Sigma-Aldrich), IIH6 (α-dystroglycan)[41], Rabbit 83 (β-dystroglycan)[42], Rabbit 229 (δ-sarcoglycan)[43], and Rabbit 256 (sarcospan)[44]. Monoclonal antibodies Ad1/20A6 (α-sarcoglycan), βSarc1/5B1 (β-sarcoglycan), and 35DAG/21B5 (γ-sarcoglycan) were generated in collaboration with L.V.B. Anderson (Newcastle General Hospital, Newcastle upon Tyne, UK). For the ε-sarcoglycan antibody (Rabbit 284), rabbit polyclonal antibodies were generated in New Zealand white rabbits intramuscularly and subcutaneously injected with a C-terminal mouse ε-sarcoglycan peptide (C-QTQIPQPQTTGKWYP) covalently linked to BSA. Antibody specificity was verified by competition experiments with the corresponding peptide on immunoblots. KCl-washed skeletal muscle membranes were prepared and immunoblot analysis was performed as described previously[10]. Immunofluorescence was performed on 7-μm transverse cryo sections as previously described[4]. Evans blue dye injections and exercise experiments were performed as described previously[4, 45].

Acknowledgements for supporting online material
Contractile properties (Supporting online material) were measured in the Contractility Core of Nathan Shock Center (J.A.F.).

References for supplementary material

1. Harper, S. Q. et al. Modular flexibility of dystrophin: implications for gene therapy of Duchenne muscular dystrophy. Nat Med 8, 253-61 (2002).
2. Scime, A. & Rudnicki, M. A. Molecular-targeted therapy for duchenne muscular dystrophy : progress and potential. Mol Diagn Ther 12, 99-108 (2008).
3. Fadel, P. J., Zhao, W. & Thomas, G. D. Impaired vasomodulation is associated with reduced neuronal nitric oxide synthase in skeletal muscle of ovariectomized rats. J Physiol 549, 243-53 (2003).
4. Duclos, F. et al. Progressive muscular dystrophy in alpha-sarcoglycan-deficient mice. J Cell Biol 142, 1461-71. (1998).
5. Grady, R. M. et al. Role for alpha-dystrobrevin in the pathogenesis of dystrophin-dependent muscular dystrophies. Nat Cell Biol 1, 215-20 (1999).
6. Pomplun, D., Mohlig, M., Spranger, J., Pfeiffer, A. F. & Ristow, M. Elevation of blood glucose following anaesthetic treatment in C57BL/6 mice. Horm Metab Res 36, 67-9 (2004).
7. Raisis, A. L. Skeletal muscle blood flow in anaesthetized horses. Part II: effects of anaesthetics and vasoactive agents. Vet Anaesth Analg 32, 331-7 (2005).
8. Voikar, V., Polus, A., Vasar, E. & Rauvala, H. Long-term individual housing in C57BL/6J and DBA/2 mice: assessment of behavioral consequences. Genes Brain Behav 4, 240-52 (2005).
9. Crosbie, R. H. et al. mdx muscle pathology is independent of nNOS perturbation. Hum Mol Genet 7, 823-9 (1998).
10. Durbeej, M. et al. Disruption of the beta-sarcoglycan gene reveals pathogenetic complexity of limb-girdle muscular dystrophy type 2E. Mol Cell 5, 141-51 (2000).
11. Lynch, G. S. et al. Contractile properties of diaphragm muscle segments from old mdx and old transgenic mdx mice. Am J Physiol 272, C2063-8 (1997).
12. Anderson, J. E. & Vargas, C. Correlated NOS-Imu and myf5 expression by satellite cells in mdx mouse muscle regeneration during NOS manipulation and deflazacort treatment. Neuromuscul Disord 13, 388-96 (2003).
13. Anderson, J. E., Weber, M. & Vargas, C. Deflazacort increases laminin expression and myogenic repair, and induces early persistent functional gain in mdx mouse muscular dystrophy. Cell Transplant 9, 551-64 (2000).
14. Archer, J. D., Vargas, C. C. & Anderson, J. E. Persistent and improved functional gain in mdx dystrophic mice after treatment with L-arginine and deflazacort. Faseb J 20, 738-40 (2006).
15. St-Pierre, S. J. et al. Glucocorticoid treatment alleviates dystrophic myofiber pathology by activation of the calcineurin/NF-AT pathway. Faseb J 18, 1937-9 (2004).
16. Hougee, S. et al. Oral administration of the NADPH-oxidase inhibitor apocynin partially restores diminished cartilage proteoglycan synthesis and reduces inflammation in mice. Eur J Pharmacol 531, 264-9 (2006).
17. Glowka, F. K. Stereoselective pharmacokinetics of ibuprofen and its lysinate from suppositories in rabbits. Int J Pharm 199, 159-66 (2000).
18. Gupta, M., Kovar, A. & Meibohm, B. The clinical pharmacokinetics of phosphodiesterase-5 inhibitors for erectile dysfunction. J Clin Pharmacol 45, 987-1003 (2005).

19. Takimoto, E. et al. Chronic inhibition of cyclic GMP phosphodiesterase 5A prevents and reverses cardiac hypertrophy. Nat Med 11, 214-22 (2005).
20. Walker, D. K. et al. Pharmacokinetics and metabolism of sildenafil in mouse, rat, rabbit, dog and man. Xenobiotica 29, 297-310 (1999).
21. Asai, A. et al. Primary role of functional ischemia, quantitative evidence for the two-hit mechanism, and phosphodiesterase-5 inhibitor therapy in mouse muscular dystrophy. PLoS ONE 2, e806 (2007).
22. Crosbie, R. H. et al. Membrane targeting and stabilization of sarcospan is mediated by the sarcoglycan subcomplex. J Cell Biol 145, 153-65 (1999).
23. Kameya, S. et al. alpha1-syntrophin gene disruption results in the absence of neuronal-type nitric-oxide synthase at the sarcolemma but does not induce muscle degeneration. J Biol Chem 274, 2193-200 (1999).
24. Eu, J. P. et al. Concerted regulation of skeletal muscle contractility by oxygen tension and endogenous nitric oxide. Proc Natl Acad Sci U S A 100, 15229-34 (2003).
25. Kinugawa, S. et al. Limited exercise capacity in heterozygous manganese superoxide dismutase gene-knockout mice: roles of superoxide anion and nitric oxide. Circulation 111, 1480-6 (2005).
26. Thomas, G. D. et al. Impaired metabolic modulation of alpha-adrenergic vasoconstriction in dystrophin-deficient skeletal muscle. Proc Natl Acad Sci U S A 95, 15090-5 (1998).
27. Wang, M. X. et al. Nitric oxide in skeletal muscle: inhibition of nitric oxide synthase inhibits walking speed in rats. Nitric Oxide 5, 219-32 (2001).
28. Seddon, M. D., Chowienczyk, P. J., Brett, S. E., Casadei, B. & Shah, A. M. Neuronal Nitric Oxide Synthase Regulates Basal Microvascular Tone in Humans In Vivo. Circulation, CIRCULATIONAHA.107.744540 (2008).
29. Perretti, M. & Ahluwalia, A. The microcirculation and inflammation: site of action for glucocorticoids. Microcirculation 7, 147-61 (2000).
30. Chao, D. S., Silvagno, F. & Bredt, D. S. Muscular dystrophy in mdx mice despite lack of neuronal nitric oxide synthase. J Neurochem 71, 784-9 (1998).
31. Wehling, M., Spencer, M. J. & Tidball, J. G. A nitric oxide synthase transgene ameliorates muscular dystrophy in mdx mice. J Cell Biol 155, 123-31 (2001).
32. Punkt, K. et al. Nitric oxide synthase is up-regulated in muscle fibers in muscular dystrophy. Biochem Biophys Res Commun 348, 259-64 (2006).
33. Cohn, R. D. et al. Prevention of cardiomyopathy in mouse models lacking the smooth muscle sarcoglycan-sarcospan complex. J Clin Invest 107, R1-7 (2001).
34. Tsunoda, M., Takezawa, K., Yanagisawa, T., Kato, M. & Imai, K. Determination of catecholamines and their 3-O-methyl metabolites in mouse plasma. Biomed Chromatogr 15, 41-4 (2001).
35. Barbato, J. C. Nicorandil: the drug that keeps on giving. Hypertension 46, 647-8 (2005).
36. Miki, T. et al. Mouse model of Prinzmetal angina by disruption of the inward rectifier Kir6.1. Nat Med 8, 466-72 (2002).
37. Stamler, J. S. & Meissner, G. Physiology of nitric oxide in skeletal muscle. Physiol Rev 81, 209-237 (2001).

38. Johnson, J. E., Wold, B. J. & Hauschka, S. D. Muscle creatine kinase sequence elements regulating skeletal and cardiac muscle expression in transgenic mice. Mol Cell Biol 9, 3393-9 (1989).
39. Sigmund, C. D. et al. Regulated tissue- and cell-specific expression of the human renin gene in transgenic mice. Circ Res 70, 1070-9 (1992).
40. Duclos, F. et al. Progressive muscular dystrophy in alpha-sarcoglycan-deficient mice. J Cell Biol 142, 1461-71 (1998).
41. Ervasti, J. M. & Campbell, K. P. Membrane organization of the dystrophin-glycoprotein complex. Cell 66, 1121-31 (1991).
42. Williamson, R. A. et al. Dystroglycan is essential for early embryonic development: disruption of Reichert's membrane in Dag1-null mice. Hum Mol Genet 6, 831-41 (1997).
43. Roberds, S. L., Anderson, R. D., Ibraghimov-Beskrovnaya, O. & Campbell, K. P. Primary structure and muscle-specific expression of the 50-kDa dystrophin-associated glycoprotein (adhalin). J Biol Chem 268, 23739-42. (1993).
44. Lebakken, C. S. et al. Sarcospan-deficient mice maintain normal muscle function. Mol Cell Biol 20, 1669-77. (2000).
45. Straub, V. et al. epsilon-sarcoglycan replaces alpha-sarcoglycan in smooth muscle to form a unique dystrophin-glycoprotein complex. J Biol Chem 274, 27989-96. (1999).